Case Studies in Construction Materials 3 (2015) 70–77

Contents lists available at ScienceDirect

Case Studies in Construction Materials

journal homepage: www.elsevier.com/locate/cscm

Case study

Self-monitoring application of conductive asphalt concrete under indirect tensile deformation

Xiaoming Liu[a,*], Zhihong Nie[a], Shaopeng Wu[b], Cui Wang[a]

[a] School of Civil Engineering, Central South University, Changsha 410075, China
[b] State Key Laboratory of Silicate Materials for Architectures, Wuhan University of Technology, Wuhan 430070, China

ARTICLE INFO

Article history:
Received 24 March 2015
Received in revised form 29 June 2015
Accepted 14 July 2015
Available online 23 July 2015

Keywords:
self-monitoring
conductive
asphalt concrete
indirect tensile deformation
CT identification

ABSTRACT

Conductive asphalt concrete has excellent self-monitoring abilities for internal damage and attractive application prospects. By studying the resistance and strain changes under indirect tensile deformation, three distinct stages of output resistivity changes are observed during the destruction of the specimen. In the initial loading stages, contact between the mixture particles tightens because the specimen under loading forms a more conductive path, and the resistivity decreases significantly. In the second stage, asphalt concrete deforms smoothly; small changes in the interior of the asphalt concrete also correspond to small changes in resistivity. In the final stage, because of the progressive development of cracks in asphalt concrete, the specimens are destroyed, and the conductive paths are also seriously damaged, significantly increasing resistivity. This change in the resistivity value exceeds 50%. Conductive asphalt concrete also has a good self-monitoring ability regarding the strain caused by the applied stress. The unit strain corresponding to changes in resistivity is greater when graphite content is lower. CT (Computer Tomography)identification can confirm that changes in resistivity are caused by material changes in the interior due to fatigue failure. The decrease or increase in resistivity is the result of a decrease or increase in the internal porosity of the material.

1. Introduction

Conductive asphalt concrete can be prepared by adding a conductive material such as graphite powder, carbon fibre, or blast furnace carbon black to ordinary asphalt concrete. The conductive properties are thus changed; resistance can decrease from $10^{13}\ \Omega$ to $10^{2}\ \Omega$ or even less (Wen and Chung, 2004, 2005; Wu et al., 2002, 2003, 2005; Liu and Wu, 2010; 2011a,b). This modified conductive concrete also has superior smart characteristics (Liu et al., 2008, 2009; Wu et al., 2003) and road performance and is used in roads, bridges or airport runways; the material is expected to self-monitor stress, strain and defects.

Self-monitoring asphalt concrete is a structural material that does not require implantation or addition of sensors and has the following advantages:

* Corresponding author at: School of Civil Engineering, Central South University, 22# Shaoshan South Road, Changsha 410075, Hunan Province, China. Fax: +86 82656263.
E-mail address: 122249300@qq.com (Z. Nie).

http://dx.doi.org/10.1016/j.cscm.2015.07.002
2214-5095/

1) The embedding of sensors and resulting performance degradation can be avoided.
2) The material self-monitors its structure at a low cost.
3) Accuracy and timeliness.
4) Stable performance and high durability.

In addition, asphalt concrete strain self-monitoring can be applied in weighing (strain-stress correspondence) and confirming the overloading of vehicles, traffic monitoring and structural vibration control (strain correspondence to vibration) (Liu and Wu, 2008). Previous reports showed that (Liu et al., 2009a,b; Liu and Wu, 2011a,b) conductive asphalt composites containing graphite powder can monitor cycle load strain under uniaxial compression.

There are several indoor fatigue tests for asphalt mixtures. Currently, the most widely used methods are the simple bending test, support bending test, uniaxial test, indirect tensile test, triaxial test, fracture mechanics testing and rutting test. According to the SHRP, comparing the advantages and disadvantages of the fatigue test method (Superpave Mix Design, 1996; AASHTO, 2015), the repeated bending and indirect tensile tests are better comprehensive evaluations and have been widely adopted. However, beam specimens are difficult to produce and are influenced by unstable factors, and the test methods are complex and produce widely varying results. In contrast, cylindrical specimens are more conveniently produced, and the test methods are simple and easily performed; therefore, this paper introduces the self-monitoring applications of conductive asphalt concrete to the indirect tensile test through changes in resistance of the strain and fatigue damage of the material.

Damage mechanics (Li and Zhang, 2003) is a new discipline established in the 1980s that focuses on the occurrence and development of microscopic defects, microcracks, and micropore points (which, taken collectively, are injurious) before the appearance of macroscopic cracks. Asphalt concrete is a complex heterogeneous composite whose damage mechanism is the basis of the study of asphalt concrete damage. Determination of the law between internal damage and the variation of resistivity is the foundation of damaging self-monitoring conductive asphalt concrete. This method is an effective way to study injury and damage accumulation through analysis of the interior of asphalt concrete.

CT (computer tomography) technology displays high-resolution digital images of different densities of information at a specified level in computer image reconstruction. In the process of X-ray penetration of substances, the intensity decay is exponential. The density of the material is evidenced by the X-ray attenuation coefficient, which differs for different substances. When an X-ray penetrates a detected object, the light intensity is defined as follows:

$$I = I_0 \exp(-\mu_m \rho_x) \quad ,$$

where I_0 is the light intensity of X-rays before penetrating the object; I is the light intensity of X-rays after penetrating the object; μ_m is the detected mass absorption coefficient per unit, which is only related to the wavelength of the incident X-ray under normal circumstances; x is the penetration length of the incident X-ray; and ρ is the material density. Therefore, the following equation for the X-ray absorption coefficient is more convenient:

$$\mu = \mu_m \rho \mathrm{cm}^{-1} \quad .$$

For water, ρ = 1.0; thus, for its absorption coefficient, $\mu_w = \mu_m$.

The CT number is the CT quantitative description; the CT numbers of air, water and ice are defined as −1000, 0 and −100. The X-ray absorption coefficient can be converted to the CT number by the following relationship:

$$\mathrm{CT}_{\mathrm{number}} = \frac{\mu - \mu_w}{\mu_w} \times 1000 \quad ,$$

where μ_w is the X-ray absorption coefficient for water. A complete set of CT images can be obtained because brightness is proportional to the CT number. The differences and changes in material composition and damage can be detected by the CT number and CT images.

Table 1
Materials and properties descriptions.

Materials	Descriptions
Asphalt binder (AH-70)	Asphalt with a penetration of 65 (0. mm at 25 °C, 100 g and 5 s), ductility of 167.3 cm (at 5 °C) and softening point of 45.4 °C
Graphite	Its particle size <150 μm, carbon content 98.9%, ash content 0.2%, iron content 0.03% by weight, the electrical resistivity $10^{-4}\,\Omega$ cm
Carbon fiber	Its tensile strength 1.68 GPa, tensile modulus 752 GPa, fiber diameter 10 μm, and average filament length 5 mm, the electrical resistivity $10^{-3}\,\Omega$ cm
Aggregate	A crashed basalt mineral, with a density of 2.93 g/cm^3 and the maximal size of 19 mm, their electrical resistivity was more than $10^{14}\,\Omega$ cm. Limestone powders were applied as the mineral filler, with a density of 2.830 g/cm^3 and major chemical compounds: CaO content 51.5% and SiO_2 content 1.76%. The passed percentage on sieve was 100%, 97.3% and 83.7 % for the sieve openings 0.3 mm, 0.15 mm and 0.07 5mm, respectively

In the early 1990s, the U.S. Highway Development Strategic Research Program (SHRP) examined the internal structure of asphalt mix core samples using CT technology (Li and Zhang 2005a,b). Masad et al. (Li and Zhang 2005a,b), using CT technology with digital camera technology, have quantitatively analysed the compaction effect and the internal structure of the mixture specimens of different compaction modes. CT scans and indirect tensile tests can be used to explore the calculation of the damage variable at different loading and unloading stages. The injury development, evolution equations and intensity attenuation law are the basis of asphalt concrete damage self-monitoring.

2. Experimental methods

2.1. Raw materials

The materials and their properties are shown in Table 1.

In this study, the Superpave12.5 composition was prepared for electrical resistivity measurements, and indirect tensile test specimens are shown in Table 2. The aggregates were a mixture of 23% crushed stone (4.75–9.5 mm), 72% fine crushed stone (<2.36 mm) and 5% fillers (<0.075 mm) by weight, which was 4.2–5.2% for asphalt. Three specimens of each composition were prepared by a gyrate compactor (EP-31111 model, America) at a temperature of 155 ± 1 °C. Gyrate numbers are $N_{ini} = 9$, $N_{des} = 125$, and $N_{max} = 205$ (SHRP-A-656., 1993). The size of the specimen is 150 ± 5 mm in diameter and 130 ± 5 mm in height.

2.2. Preparation of specimen

In this study, two specimens of each group with the same composition were prepared by gyrate compactor (EP-31111 model, America) at the temperature of 155 ± 1 °C. The gyrate number was $N_{ini} = 9$, $N_{des} = 125$, and $N_{max} = 205$. The size of the samples was $\Phi 150 \times (130 \pm 5)$ mm. When the mixture was fed into the mold, two wire-mesh (70 mm × 70 mm sieve; 5 mm × 5 mm sieve) electrodes were pre-imbedded on both sides of the samples.

2.3. Test methods

2.3.1. ITT test

Testing was performed at 15 °C under cyclic indirect tensile testing. A hydraulic mechanical testing system (UTM-25, Australia) was used until the specimens were totally destroyed. During mechanical testing, the longitudinal strain was measured with a strain gauge. Three specimens of each composition were tested to ascertain reproducibility of the trends reported here.

2.3.2. Electrical measurements

Simultaneous with mechanical testing, electrical resistance measurements were made by a Keithley 2700 multimeter (USA). Resistance measurement of specimen in indirect tensile test are shown in Fig. 1. Changes in the specimen longitudinal displacement and resistance should be recorded, during the load test.

The reading frequency of resistance was equal to that of loading (10 Hz). The longitudinal strain and resistance were measured simultaneously for each specimen. Technical details can be found elsewhere (Zhonghe, 1995). The four-probe method was used for specimens of resistivity approximately $10^5\,\Omega$ cm or less. The outer two electrical contacts (40 mm apart) were for passing current, and the inner two electrical contacts were for voltage measurement. Each of the two pairs of electrical contacts was symmetrically positioned relative to the mid-point of the specimen length. Each electrical contact was around the entire perimeter of the specimen in a plane perpendicular to the specimen length. The two-probe method was used for specimens of resistivity beyond $10^6\,\Omega$ cm. Six specimens of each type were tested. Technical details can be found elsewhere (Taya et al., 1998).

Table 2
Superpave 12.5 (passage%).

Sieve size (mm)	19	12.5	9.5	4.75	2.36	1.18	0.6	0.3	0.15	0.075
Gradation	100	95.6	77.3	49.5	29.7	21.7	15.7	10.5	7.9	5.7
Maximum	100	92	80	62	48	36	26	18	14	8
Minimum	100	76	60	34	20	13	9	7	5	4

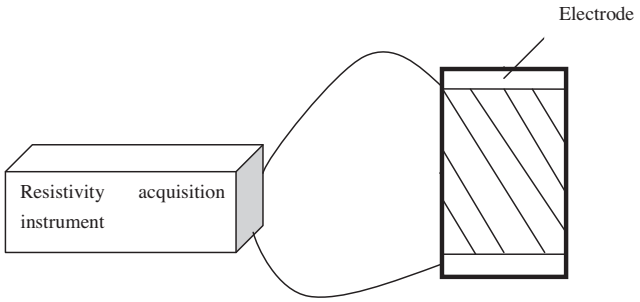

Fig. 1. The schematic representation of resistance measurement of cylinder specimen.

3. Results and discussion

3.1. Self-monitoring studies under uniaxial compression

Previous studies have shown that conductive asphalt concrete responds well to load (stress) and strain because the change of resistivity is due to a change in the internal structure of graphite particles and spacing of carbon fibres. The conductive asphalt concrete structure is thus damaged. The internal conductive network is also affected, which is bound to affect a change in resistance. Correspondence of this change to damage and application to actual engineering would bring enormous economic and social benefits.

Previously used Superpave12.5 gradations described the specimen with added 22.5 vol% graphite and 1.0 vol% carbon fibre. The loading frequency was 10 Hz, the maximum load 4 kN and the minimum load 200 N. Continuous loading and stress control mode was used, and the test temperature was 20 °C. Fig. 1 shows the resistivity and longitudinal displacement variation curve during dynamic load until complete destruction of conductive asphalt concrete, in which resistivity is the thick curve, and strain is the thin curve. Three distinct stages in the variation of resistivity are observed in the process of specimen destruction. In the first stage, the initial stage of the load (at 1.0% of the fatigue lifetime), the conductive asphalt concrete specimens have much closer contact between the mixture and form a more conductive path; thus, resistivity declines sharply. The fractional change in the resistivity of this process is approximately 70%. In the second stage, asphalt concrete specimens are in a smooth deformation process, accounting for 80% of the fatigue lifetime (from 1% to 82%); there is little change in the internal structure of asphalt concrete, and the change in resistivity is also small. The total process of change in resistivity does not exceed 10%. In the final stage, due to progressive development of microcracks in the asphalt concrete, the specimens are completely destroyed, and the conductive paths are also seriously damaged; thus, resistivity increases sharply. This process accounts for approximately 20% of the fatigue life, and the change in resistivity is greater than 50%.

If the conservation programs of asphalt pavement at the conservative point shown in Fig. 2 were used and the optimal maintenance time were considered, maintenance costs could be reduced and the asphalt pavement lifetime significantly extended. When damage is found in its early stages, and related solutions are proposed, the pavement performance index can be restored to the original 90% to 100%, significantly extending road lifetime. Existing manual inspection typically

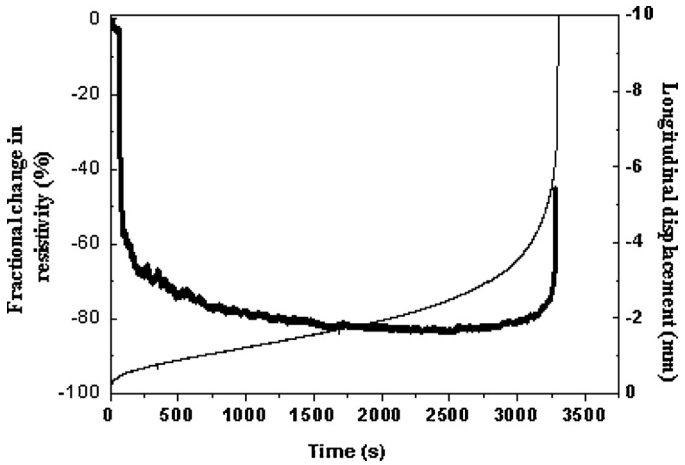

Fig. 2. Curves of the resistivity (thick curve) and longitudinal displacement variation (thin curve) during the dynamic load.

assumes that the proposed conservation in asphalt pavement performance index dropped to 30–40% and that the recovery can only stay between 40 and 60% of the original level. Self-monitoring techniques can maximise protection of normal service functions and reduce maintenance costs and thus is an ideal nondestructive testing technology.

3.2. Self-monitoring studies under indirect tensile deformation

3.2.1. Self-monitoring study with different conductive material contents

Conductive asphalt concrete has highly piezoresistive characteristics under uniaxial compression, according to previous reports. The resistance varies with compression stress and tensile stress. This paper focuses on a cylindrical specimen with different conductive material contents, different loads, and different temperatures of external load caused by the stress/strain behaviour of self-monitoring under indirect tensile deformation.

Superpave12.5 gradations used previously described the specimen with additional 22.5 vol% graphite and 1.0 vol% carbon fibre, with initial resistivity if 84 37 Ω cm. Fig. 3 shows the resistivity and change curve of strain under the indirect tensile test in stress control mode. The maximum and minimum loads were 4 kN and 200 N, respectively; the waveform was a half-sine, and the test temperature was 20 °C. The change in resistance and longitudinal deformation of the specimen was recorded under loading. The resistance reading counts were six times per second.

As shown in Fig. 2, the resistance increases as the strain increases reversibly and decreases as the strain recovers. The resistivity changes indicate negative piezoresistivity, that is, the resistivity decreases as the load increases and returns to the initial state after unloading. Because of the influence of noise and changes in the structure, the variation of the absolute value of each cycle in resistivity may not be consistent. However, the changes in resistivity of frequency and load frequency are equal, meaning that the resistivity of each cycle changes in response.

Fig. 4 shows a similar relationship to Fig. 3, but the graphite content is reduced to 15 vol% of the specimens in Fig. 4, with all other conditions being the same. The sensitivity of the resistivity deformation is higher than in the first case. Graphite content is relatively low, and the carrier concentration of the unit volume change is larger than that of the high-graphite-content case; thus, greater unit strain corresponds to a change in resistivity value, which results in higher sensitivity.

The changes in resistivity and the structure of each cycle in response can be explained by the conductive mechanism (Zhang, 1995). When mixing graphite and carbon fibre content exceeds the percolation threshold, the conductivity of the conductive concrete mechanism is controlled by the contact mechanism (Sihai and Chung, 1999). When a load is applied on the conductive asphalt concrete specimens, resulting in closer contact between the graphite particles and between graphite and carbon fibre, a more conductive path is formed, and the resistivity thus decreases. When unloaded, due to elastic recovery, the distance between the graphite particles and between graphite and carbon fibre is also restored to the original value; hence, the resistivity is also restored to its initial value. However, because resistivity is also affected by noise and structural changes in the loading process, the absolute value of resistivity is different for each cycle.

When its graphite content is low, conductive asphalt concrete contains a relatively small number of conductive particles per unit volume. The change in resistivity caused by loading is higher when graphite content is lower. The piezoresistive mechanism of conductive asphalt concrete has been previously studied (Liu and Wu, 2014). The resistivity of conductive asphalt concrete is related to its internal carrier concentration; the density of the conductive material per unit volume increases after asphalt concrete is compacted, and the resistivity decreases. Thus, the self-monitoring capacity is relatively low when the conductive material content is high.

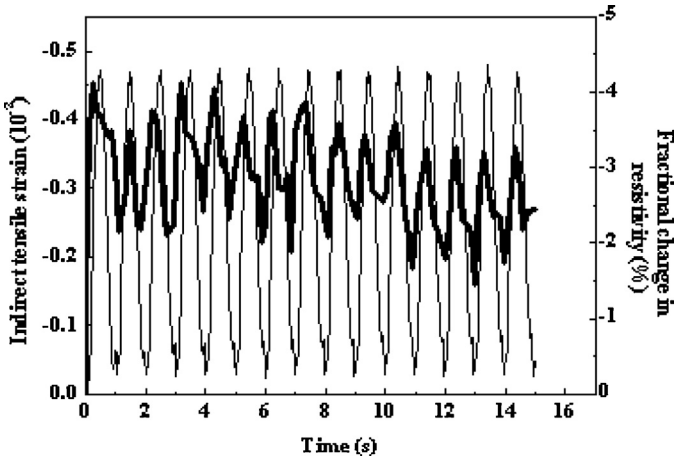

Fig. 3. The resistivity (thick curve) and change curve of strain (thin curve) under the indirect tensile test in the stress control mode for the asphalt concrete with 22.5% graphite particle and 1.0% carbon fiber as the filler.

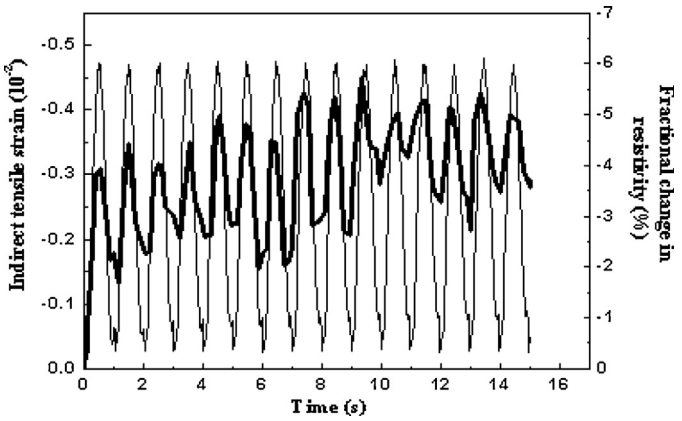

Fig. 4. The resistivity (thick curve) and change curve of strain (thin curve) under the indirect tensile test in the stress control mode for the asphalt concrete with 15% graphite particle and 1.0% carbon fiber as the filler.

Higher smartness cannot be obtained by simply reducing the graphite material content; the resistance is significantly decreased only when the conductive material content is greater than its percolation threshold, but the decrease of resistivity is small when its content is greater than 20 vol%. Thus, the graphite content should be controlled at between 15 and 20% for available sensitivity. The material has ideal sensitivity coefficients only when graphite content is in the range of the threshold value.

3.3. CT identification of damage

We used the indirect tensile repeated loading and unloading fatigue test combined with CT scans to observe changes in the internal structure of the specimen. The equipment used was a UTM-25 dynamic material testing system and multislice spiral CT scan machine. Specimens were formed by rotation. Sample diameter and height were 150 mm and 106 mm, respectively; the selected slice thickness was 3-mm layers and interval of 3 mm, and scanning voltage and current were 120 kV and 300 mA, respectively. In selected scan conditions, the expansion process of cracks during fatigue tests was observed. The fatigue damage is divided into three different stages of four scans, with a typical scanning image shown in Fig. 5. The change in resistivity during the fatigue process and longitudinal displacement curve are shown in Fig. 6

3.4 *Damage analyses of specimen internal structure*

We used different CT image processing methods to analyse asphalt concrete mesostructure damage evolution. Applying the K-means law with WIT image processing software, we obtained the void change in the scan surface of the specimens. This change and the change in resistivity are plotted in Fig. 6.

Fig. 6 indicates that the internal structure of the asphalt mixture goes through the following three stages in the indirect tensile fatigue test process. First, the porosity decreases in the initial loading, and contact between the aggregates becomes closer (Fig. 5b and Fig. 6A and B); thus, the resistivity declines. With increased loading, injury begins to appear, and the internal porosity of the mixture is gradually increased (Fig. 5c and Fig. 6C and D); resistivity increases slightly, microdamage slowly grows and larger cracks expand in the loading stage. The porosity of the mixture increases rapidly, and the specimen is destroyed (Fig. 5d and Fig. 6D and E). The resistivity increases dramatically, which fully indicates that mixed resistivity change is due to porosity changes caused during the fatigue test process. These results demonstrate resistivity changes in the

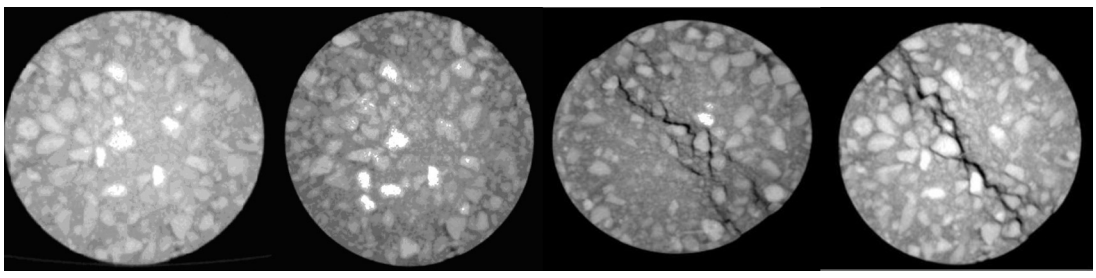

Fig. 5. CT photograph of different fatigue periods.

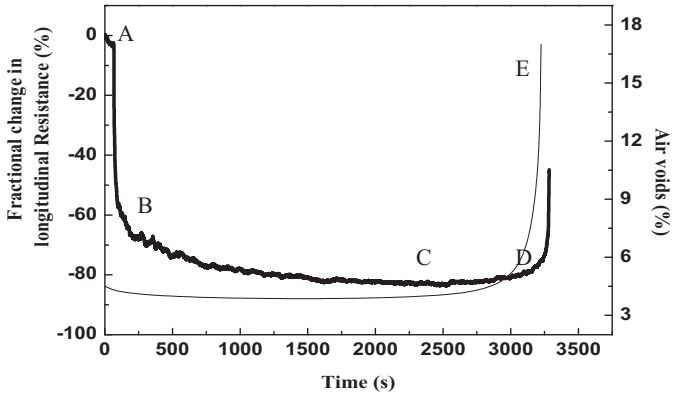

Fig. 6. The change in resistivity (thick curve) during the fatigue process and longitudinal displacement curve (thin curve).

fatigue process but also give information about the changes in the internal structure of the mixture to achieve a true sense of the self-monitoring effect.

The smart characteristics of conductive asphalt concrete can be applied as a strain or stress sensor that is mainly used in pressure sensing of aircraft and vehicles and civil engineering applications such as bridge vibration sensors. The most intuitive explanation of smart properties is that a conductive network is formed by the overlap of conductive particles. Such a material can be conductive only when the conductive particles are within a certain distance from one another. When the conductive particles are further apart than this distance, the conductivity between them fails, so this distance is a valid distance. Strain changes the gap between conductive particles and thus affects the resistivity of the system. The gap between conductive particles increases with applied tensile stress, thus increasing resistivity. With applied pressure, the gap between conductive particles shortens, and resistivity decreases. These explanations only deal with the gap changes of conductive particles. With further research, some different mechanisms, such as the effects of boundary and microcracks may also be introduced. In short, the dependence of resistance on stress is related to the destruction and reorganisation of the conductive network.

The smart features of conductive asphalt concrete are attractive. Compared to other embedded-sensor smart materials, conductive asphalt concrete does not require an embedded internal sensor but can sense its own strain or stress. The material responds in a timely manner, has low cost, good durability, and perceived ability, and its characteristics are not degraded due to an implanted external sensor.

4. Conclusions

Conductive asphalt concrete with a suitable amount of graphite powder and carbon fibre can effectively diagnose its own strain during the loading process and resulting damage.

(1) The resistivity changes are a negative pressure resistance effect in which resistivity decreases as the load increases and back to the initial state after unloading. Although the variation of the absolute value of each cycle in resistivity may not be consistent because of the influence of noise and changes in the structure, the changes in the resistivity of frequency and load frequency are equal, demonstrating that the resistivity of each cycle changes in response.
(2) Conductive asphalt concrete has excellent self-monitoring capabilities of internal damage, and there are three distinct stages of resistivity changes during the destruction process of the specimen. In the initial stages of loading, the contact between the mixture becomes tighter because the conductive asphalt concrete specimen is subjected to loads, forming a more conductive path, and the resistivity decreases sharply. In the second stage, asphalt concrete is deformed smoothly. In this process, small changes in the internal structure of the asphalt concrete result in small changes in resistivity. In the final stage, the progressive development of cracks in asphalt concrete leads to the complete destruction of the specimen. Conductive paths are seriously damaged, resulting in a sharp increase in resistivity; the change in resistivity exceeds 50%.
(3) The resistivity change is related to internal carrier concentration. Resistivity is inversely proportional to carrier concentration. The smart mechanism is due to changes in the carrier concentration per unit volume.
(4) CT identification can confirm that resistivity change is caused by material changes in the internal structure of the process of fatigue failure. The decrease or increase in resistivity is the result of the decrease or increase of internal porosity.

References

AASHTO Designation: TP 31-96. Standard method of test for Determining the resilient modulus of bituminous mixtures by indirect tension.
Li, X., Zhang, X., 2003. Advances on dynamic discrimination of asphalt mixture damage. J. Chang'an Univ.(Natural Science Edition) 23 (6), 11–14 (in chinese).

Li, X., Zhang, X., 2005a. Internal structure discrimination of asphalt mix with X - ray computerized tomograph under repetitive uniaxial loadings. J. Harbin Instit. Technol. 37 (9), 1228–1230 (in chinese).
Li, X., Zhang, X., 2005b. Application of X-ray computerized tomography in analysis of inner structure of asphalt mix. J. Highway Transp. Res. Dev. 22 (2), 14–16.
Liu, X., Wu, S., 2008. Properties evaluation of asphalt-based composites with graphite and mine powder. Const. Build. Mater. 22 (3), 121–126.
Liu, X., Wu, S., 2010. Influence of graphite on the road performance of asphalt concrete. Wuhan Univ. Tech. (Trans. Sci. Eng.) 34 (3), 545–549 (in chinese).
Liu, X., Wu, S., 2011a. Study on the piezoresistivity character of electrically conductive asphalt concrete. Adv. Mater. Res. 233-235, 1756–1761.
Liu, X., Wu, S., 2011b. Study on the graphite and carbon fiber modified asphalt concrete. Const. Build. Mater. 25 (4), 1807–1811.
Liu, X., Wu, S., 2014. Effect of carbon fillers on electrical and road properties of conductive asphalt materials. Constr. Build. Mater. 68 (10), 301–306.
Liu, X., Wu, S., Li, N., et al., 2008. Self-monitoring application of asphalt concrete containing graphite ans carbon fibers. J. Wuhan Univ. Tech. (Mater. Sci. Ed.) 23 (2), 268–271.
Liu, X., Wu, S., Li, N., et al., 2009a. Research on the conductive asphalt concrete's piezoresistivity effect and it's mechanism. Const. Build. Mater. 23 (7), 2752–2756.
Liu, X., Wu, S., Ning, L., et al., 2009b. Smart characteristic of conductive asphalt concrete. J. Cent. South. Univ. (Sci. Tech) 40 (5), 1465–1470 (in chinese).
SHRP-A-656, 1993. Development of an Asphalt Core Tomographer. Strategic Highway Research Program. National Research Council, Washington, DC.
Sihai, W., Chung, D.D.L., 1999. Piezoresistivity in continuous carbom fiber cement-matrix composite [J]. Cem. Concr. Res. 29, 445–449.
Superpave Mix Design, Series SP 2 1996.
Taya, M., Kim, W.J., Ono, K., 1998. Piezoresistivity of a short fiberrelastomer matrix composite [J]. Mech. Mater. 28, 53–59.
Wen, S.H., Chung, D.D.L., 2004. Effects of carbon black on the thermal, mechanical and electrical properties of pitch-matrix composites. Carbon 42 (6), 2393–2397.
Wen, S.H., Chung, D.D.L., 2005. Pitch-matrix composites for electrical, electromagnetic and strain-sensing applications. J Mater. Sci. 40, 03–3897.
Wu, S., Mo, L., Shui, Z.H., Xuan, D.X., Xue, Y.J., Yang, W.F., 2002. Improvement of electrical properties of aspahlt concrete. J. Wuhan Univ. Tech. (Mate. Sci. Ed.) 17 (4), 69–72.
Wu, S., Mo, L., Shui, Z.H., 2003. Piezoresistivity of graphite modifiedasphalt concretes. Key Eng. Mater. 249, 391–395.
Wu, S., Mo, L., Shui, Z., Chen, Z., 2005. Investigation of the conductivity of asphalt concrete containing conductive fillers. Carbon 43 (7), 1358–1363.
Zhang, M., 1995. J. Mater Sci. 30, 4226–4232.
Zhonghe, S., 1995. The electrical properties of carbon fiber-cement composite (CFCC) [J]. J. Wuhan Univ. Technol. (Mater. Sci. Ed.) 10 (04), 38–42.